Japanese Journal of Applied Physics
Vol. 44, No. 3, 2005, pp. 1445–1449

Characteristics of Silicon Carbide Etching Using Magnetized Inductively Coupled Plasma

Hyo Young LEE, Dong Woo KIM, Yeon Jun SUNG[1] and Geun Young YEOM

Department of Materials Engineering, Sungkyunkwan University, Suwon, Kyunggido 440-746, Korea
[1]*M&D Lab. Samsung Advanced Institute of Technology, Suwon, Kyunggido 440-746, Korea*

(Received July 7, 2004; accepted December 6, 2004; published March 8, 2005)

In this study, SiC etching was carried out using fluorine-based magnetized inductively coupled plasmas. The SiC etch rates and etch selectivities of SiC to Cu and Ni were investigated for the purpose of obtaining high etch rates in the application of SiC etching to various optical devices and micro-electromechanical systems (MEMS). Among SF_6, CF_4 and NF_3, SF_6 showed the highest SiC etch rates and etch selectivities to Cu and Ni, due to its highest F atomic density and to the formation of nonvolatile fluoride on Cu and Ni. Cu generally showed higher etch selectivity than Ni, possibly due to the easier formation of fluoride in this case. The application of a weak axial magnetic field ranging from 0 to 80 G showed maximum SiC etch rates at 40 G, possibly due to the formation of a resonance mode. When a field of 40 G was applied, the SiC etch rate was increased approximately two times and, in this condition, the F atomic density and ion densities in the plasma were also at a maximum. The highest SiC etch rate obtained in our experiment was 2020 nm/min with an inductive power of 1400 W, a bias voltage of −600 V, a pressure of 10 mTorr of SF_6, and a magnetic field of 40 G. The etch selectivity to Ni obtained in this condition was about 40. [DOI: 10.1143/JJAP.44.1445]

KEYWORDS: inductively coupled plasma, magnetized, SiC, etching, fluorine-based gas

1. Introduction

Silicon carbide (SiC) is an excellent semiconductor material which can be used for devices operating at high power and high temperature, due to its high thermal and chemical stability.[1,2] SiC wafers are widely used as the substrates for microelectromechanical systems (MEMS) devices, due to their superior electrical and mechanical properties, and as the substrates for GaN epitaxial growth, due to the similarity of the lattice constants between GaN and SiC. In the formation of various SiC-based devices, because of its chemical stability to various wet chemicals, plasma etching is the prerequisite method for the etching of SiC. To etch SiC, especially in the case of MEMS devices, high SiC etch rates are required, in addition to a smooth etch profile and high etch selectivity to the mask materials in various processes, such as the formation of via holes, which require etching through an approximately one hundred micron thick substrate.[3–6]

To etch SiC at high rates, high density plasma sources, such as the electron cyclotron resonance (ECR) plasma, helicon plasma and inductively coupled plasma (ICP), have been investigated.[7–9] Among these different plasma sources, inductively coupled plasma sources are widely used, because of the high rate of etching that can be achieved for various materials including SiC, due to their simple source structure and physical properties, as well as their scalability to large area substrates.[3] As far as the process gas is concerned, for the high rate etching of SiC, fluorine-based gases are generally used, however, due to the low etch selectivity of SiC to photoresist, other mask materials having higher etch resistance to fluorine based gases, such as Al, indium tin oxide (ITO) and Ni, have also been used, in order to increase the etch selectivity and to obtain a smoother and more anisotropic etch profile.[10–12]

The current SiC etch rates with various fluorine-based inductively coupled plasmas reported by other researchers are generally lower than 1 μm/min, and this could be problematic in the deep etching of MEMS devices.[13,14] In this study, an inductively coupled plasma source was used to etch SiC with various fluorine-based gases and with various metal mask layers such as Ni and Cu, with the objective of obtaining high SiC etch rates and high etch selectivity over the mask materials, respectively. In addition, the possibility of obtaining higher SiC etch rates with a high etch selectivity over the mask materials by applying an axial magnetic field to the conventional ICP source was also investigated. The characteristics of the fluorine-based plasmas and their relations to the SiC etch rates were investigated using optical emission spectroscopy (OES) and quadrupole mass spectrometry (QMS).

2. Experimental Procedure

Figure 1 shows a schematic diagram of the magnetized inductively coupled plasma (MICP) etching system used in this experiment. The chamber was square shaped with an inner size of 210 mm × 210 mm and was made of anodized aluminum. Two 500 mm × 500 mm Helmholtz-type axial magnetic coils were located on the top and bottom of the chamber wall, respectively, and the distance between the coils was 285 mm. The applied magnetic field inside of the chamber varied from 0 to 100 G and the magnetic field

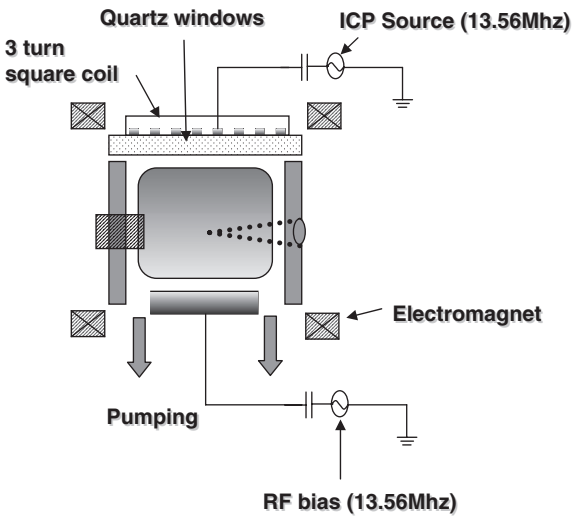

Fig. 1. Schematic diagram of MICP (magnetized inductively coupled plasma) etching system used in the experiment.

uniformity was about 3%. 13.56 MHz rf power (0–2 kW) was applied to the three turn gold coated coil located at the top of the chamber and the substrate, for the purpose of generating the inductive plasmas and dc bias voltages, respectively.

The samples used in the study were 6H-SiC generally applied as the substrates for GaN epitaxial growth. For the etch masks, a 500 nm thick Cu or Ni layer was deposited on the SiC by thermal evaporation or e-beam evaporation, respectively. The SiC samples were etched at room temperature using various fluorine-based gases, viz. SF_6, CF_4 and NF_3, with an inductive power ranging from 700 to 1400 W, a dc bias voltage ranging from -200 to -600 V, and an axial magnetic field ranging from 0 to 80 G.

The etch rates of the SiC substrate and the mask layers were measured using a step profilometer (Tencor, α-step 500). The density of the radicals was measured using OES (SC Tech, PCM420) and that of the ions in the plasmas was measured using a Langmuir probe (Hiden Analytical Inc., ESP) and using QMS (Hiden Analytical Inc., PSM500) with the view ports located on the sidewall of the chamber. The Langmuir probe used to obtain the ion density in the plasma was biased at -60 V. Ar actinometry was used for the qualitative estimation of the radical density from the observed OES intensity. For the Ar actinometry measurements, 5% Ar was added to the feed gas and the optical emission intensity ratios of F (704 nm) to Ar (750.4 nm) were calculated, in order to obtain the relative F atomic density. The QMS used in the experiment was equipped with magnetic shielded optics and, therefore, the ion signals from the plasma were not affected by the external magnetic field. The surface characteristic of the Cu mask layer, before and after its etching in a fluorine based plasma, was measured using X-ray photoelectron spectroscopy (XPS, ESCALAB-2201).

3. Results and Discussion

SiC wafers were etched with the ICP without applying a magnetic field and their etch rates were investigated using several fluorine-based gases. Figure 2(a) and 2(b) show the SiC etch rates and mask material etch rates (Cu and Ni), respectively, as a function of inductive power from 700 to 1400 W for the fluorine-based gases, SF_6, NF_3, and CF_4. The operational pressure was 10 mTorr and the dc bias voltage was maintained at -200 V. As shown in Fig. 2(a), the etch rates of SiC increased as the inductive power was increased, and, at the same inductive power, among the different fluorine-based gases, the highest etch rates were obtained with SF_6, while the lowest etch rates were obtained with CF_4. The etch rates of Cu and Ni also increased with increasing inductive power, with the exception of Cu with SF_6, in which case the growth of the mask material was observed instead of etching. In general, Cu showed lower etch rates than Ni for all of the fluorine-based gases investigated. Also, SF_6 showed the lowest mask material etch rates, even though the SiC etch rates with SF_6 were the highest. The calculated etch selectivity was infinite for SiC etching with the Cu mask in SF_6, due to the growth of the mask material, and was higher than 100 in the case of the SiC etching with the Ni mask in SF_6.

The observed increase in the SiC etch rate with increasing inductive power is related not only to the increase of the ion flux to the substrate, but also to the increase of the F atomic density in the plasma, due to the increased ionization and dissociation of the fluorine-based gas. Figure 2(c) shows the relative F atomic density measured as a function of the inductive power for SF_6, NF_3, and CF_4, as estimated by Ar actinometry using OES, and Fig. 2(d) shows the ion density measured as a function of the inductive power for SF_6 and CF_4 using a Langmuir probe. The process conditions are the same as those shown in Fig. 2(a). As shown in the figure, increasing the inductive power from 700 to 1400 W resulted not only in an approximately 100% increase in the ion density for CF_4 and SF_6, but also in increases in the relative F atomic density of approximately 40% for CF_4, 100% for SF_6, and 200% for NF_3. The increases in the SiC etch rate caused by increasing the inductive power from 700 to 1400 W, which are shown in Fig. 2(a), were approximately 100% for CF_4 and 300% for SF_6, and were therefore similar to the combined increases in the ion density and F radical density. Also, at the same inductive power, the F density and the ion density were the highest for SF_6 and the lowest for CF_4 similar to the SiC etch rates shown in Fig. 2(a). Therefore, the fact that the highest SiC etch rate was observed for SF_6 appears to be related not only to its exhibiting the highest ion density, but also the highest F atomic density, among the gases investigated in this study. The lower Cu etch rates compared to the Ni etch rates for the same gas, however, appear related to the formation of fluoride in the case of these materials.

The densities of the copper fluorides, CuF and CuF_2, are 7.1 g/cm^{-3} and 4.23 g/cm^{-3}, respectively, while that of nickel fluoride, NiF_2, is 4.7 g/cm^{-3}. Therefore, when the fluorides are formed, the density of nickel fluoride can be either similar to or lower than that of the copper fluorides. Also, the sputter yields of CuF, CuF_2 and NiF_2 by fluorine atoms at 200 eV are close to 0.57, 0.6 and 0.6, respectively, from the Stopping and Range of Ions in Matter (SRIM) calculation. Therefore, the sputter yields of the fluorides are similar to each other. However, as shown in Fig. 2(b), the growth of the Cu mask layer, rather than etching, was observed only in the case of Cu etching with SF_6, which has the highest fluorine atomic density. The growth of the Cu mask layer during the etching process appears to be caused by the rate of formation of copper fluorides being higher than their rate of removal by sputter etching. Therefore, the lower etch rates of Cu, which result in the higher etch selectivity shown in Fig. 2(b), result from the easier formation of copper fluorides as compared to that of nickel fluorides. The chemical compositions of the as-deposited Cu surfaces and those etched by SF_6 were investigated using XPS, and the results are shown in Fig. 3. As shown in this figure, the Cu 2p3/2 peaks of the Cu etched by SF_6 appeared in the form of two peaks located at 932.7 and 936.1 eV, which are believed to be from Cu and CuF_2, respectively.[15] In this figure, the peak height of Cu is higher than the peak height of CuF_2, due to the high dc bias condition. When the dc bias voltage was lower, the CuF_x peak ($x = 1, 2$) was increased and the Cu peak was decreased, due to the formation of thicker CuF_x (not shown). Therefore, during the etching of Cu, copper fluorides were formed on the Cu mask surface and the growth of the mask layer was observed.

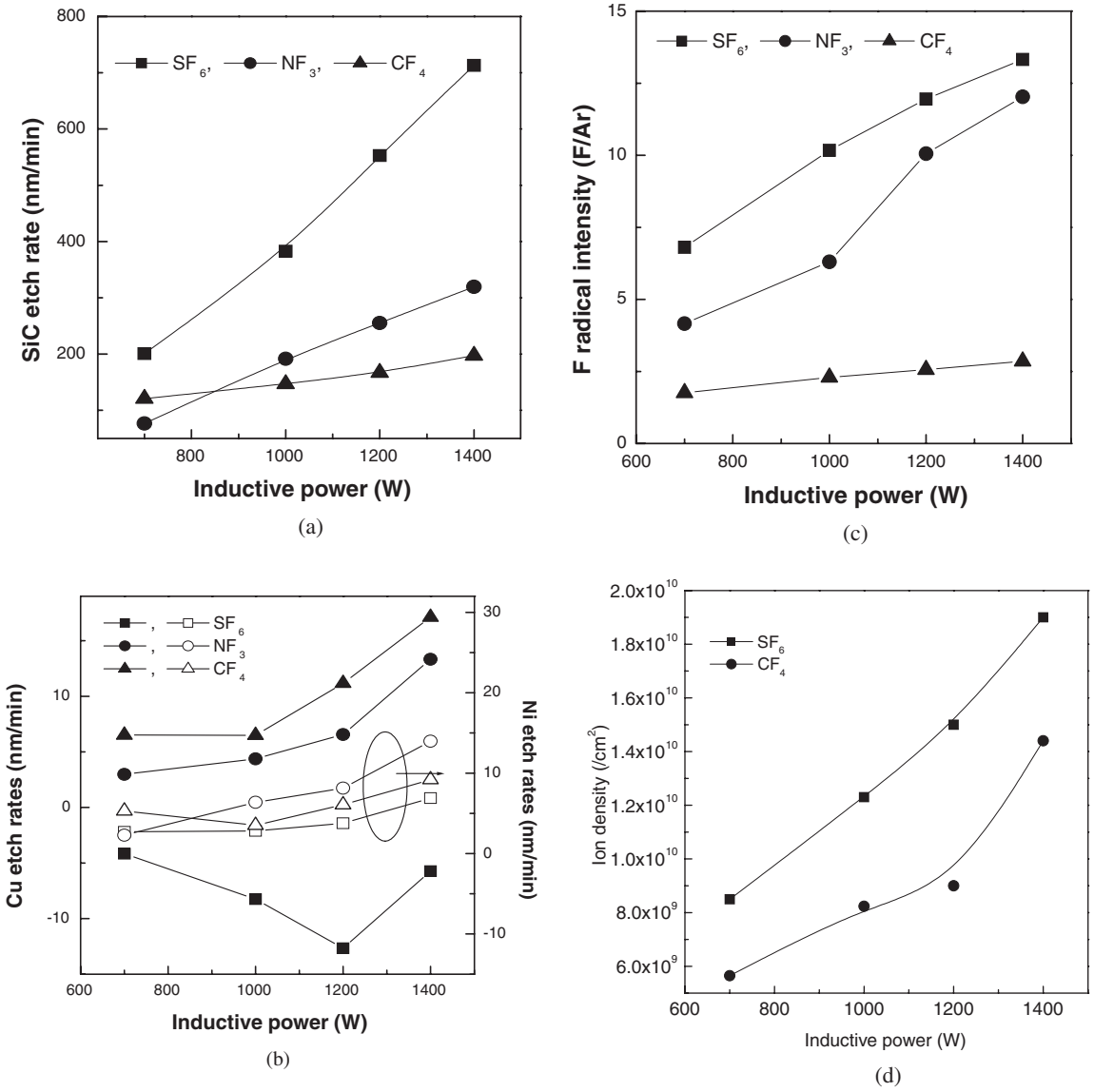

Fig. 2. SiC etch rates (a), mask material etch rates (Cu and Ni) (b), and relative F atomic density (c) measured as a function of the inductive power from 700 to 1400 W for the fluorine-based gases, SF_6, NF_3, and CF_4, at 10 mTorr and with a bias voltage of −200 V. The ion densities measured as a function of the inductive power for SF_6 and CF_4 are shown in (d).

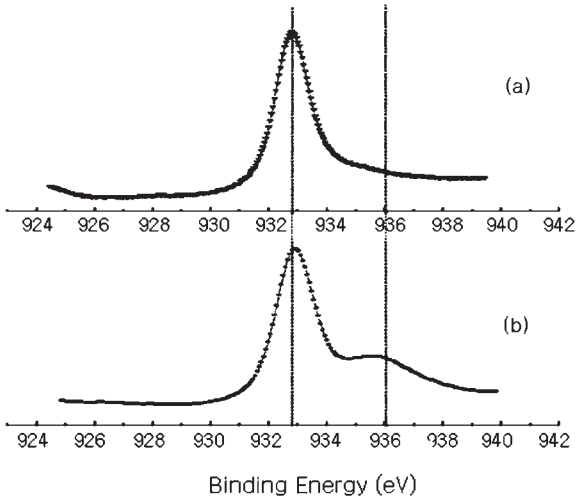

Fig. 3. X-ray photoelectron spectra of Cu 2p for (a) as-deposited Cu and (b) the Cu etched by an SF_6 inductively coupled plasma. The Cu etch condition was 10 mTorr of SF_6, an inductive power of 1400 W, a bias voltage of −600 V, and a magnetic field of 40 G.

Figure 4 shows the effect of the dc bias voltage from −200 to −600 V on the etch rates of SiC and the mask materials (Cu and Ni). The applied inductive power was 1400 W and the operational pressure was 10 mTorr with SF_6. It can be seen in this figure that, as in the case of the inductive power, the etch rates of SiC and the mask materials increased almost linearly with increasing dc bias voltage. By increasing the bias voltage from −200 to −600 V, the SiC etch rate was increased from 700 to 1200 nm/min, however, due to the increase in the mask material etch rates with increasing bias voltage, the etch selectivities were decreased from infinite to 60 for Cu and 100 to 40 for Ni. The increase in the etch rates of SiC, Cu and Ni originates from the increased ion bombardment energy. Especially, due to the greater increase in the sputter etch rates of the copper fluorides, as compared with that of the formation of the copper fluorides, the Cu mask layer changed from growth to etching during the process of etching by SF_6.

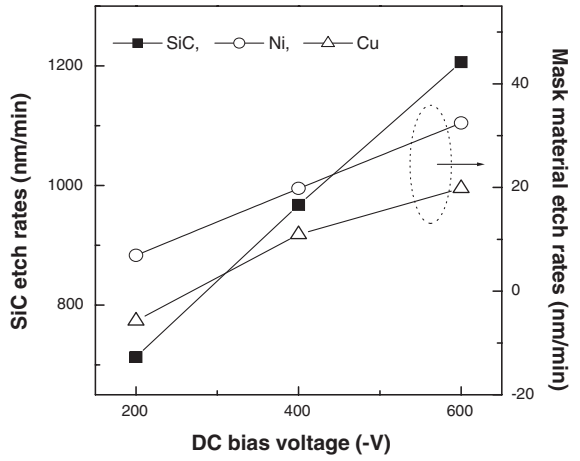

Fig. 4. SiC etch rate and mask material etch rate as a function of the bias voltage at an inductive power of 1400 W and 10 mTorr of SF_6.

Even though an increase in the SiC etch rates can be obtained by increasing the inductive power and bias voltage, the addition of a weak axial magnetic field of less than 100 G also increased the SiC etch rates. Figure 5(a) shows the etch rates of SiC and the etch selectivities over the mask materials as a function of an axial magnetic field ranging from 0 to 80 G. The inductive power, dc bias voltage and operational pressure were 1400 W, −200 V and 10 mTorr SF_6, respectively. As shown in this figure, increasing the axial magnetic field from 0 to 40 G caused the SiC etch rate to increase from 700 nm/min to 1500 nm/min, however, increasing the magnetic field further decreased the etch rate. The etch selectivities decreased continuously as the magnetic field was increased for both Cu and Ni. The etch selectivities obtained at the highest SiC etch rate were 100 for Cu and 40 for Ni.

To investigate the reason for the variation in the SiC etch rates, the relative F atomic density and SF_3^+ ion density were measured using Ar actinometry and QMS, respectively, and the results are shown in Fig. 5(b). The process conditions used for the measurements shown in Fig. 5(b) are the same as those for Fig. 5(a). As shown in Fig. 5(b), both the F atomic density and SF_3^+ ion density showed a maximum at 40 G, as in the case of the SiC etch rates. The other ion peaks, such as those for SF^+, SF_2^+, SF_4^+, F^+, etc., showed a similar trend to that of SF_3^+, even though the peak intensities for these ions were significantly lower than that for SF_3^+ (not shown). Therefore, the increase in the SiC etch rate obtained with the axial magnetic field of 40 G was related to the increased dissociation and ionization of SF_6. This increased dissociation and ionization caused by the application of a magnetic field of 40 G appear to be related to the formation of some kind of resonance mode during the operation of an inductively coupled plasma with a weak magnetic field. In fact, the application of a weak axial magnetic field can increase the helical motion of energetic electrons and reduce the loss of energetic electrons to the chamber sidewall, thereby resulting in an increase in the radical and ion density in plasma. However, the further increase in the axial magnetic field could interfere with the circular electric field generated by the inductive power and reduce the densities by distorting the electric Even though

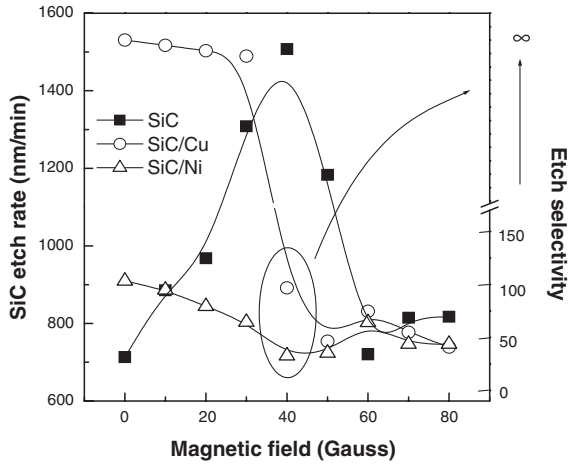

(a)

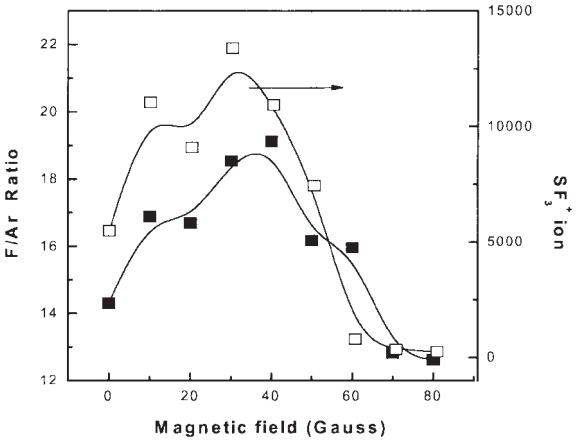

(b)

Fig. 5. SiC etch rates and mask material etch selectivities (a) and relative F atomic density and ion density measured by OES and QMS, respectively (b) as a function of the magnetic field at an of inductive power of 1400 W, a bias voltage of −200 V, and 10 mTorr of SF_6.

the exact reason for the increased dissociation and ionization obtained with a weak magnetic field is not currently known, the benefit of the magnetic field can be seen by comparing the SiC etch rates and etch selectivities shown in Fig. 5(a) with those in Fig. 4. Due to the high binding energy of SiC, even though the Si and C in SiC can be easily removed by F atoms through the formation of volatile SiF_x and CF_x, the bonding of SiC has to be broken by the ion bombardment for the SiC etching. By the application of a weak magnetic field, both the ion density and F atomic density were able to be increased at a fixed inductive power. Therefore, high SiC etch rates could be obtained through both the increased breakage of SiC bonds, resulting from the increased ion flux, and the increased formation of volatile SiF_x and CF_x resulting from the increased F atomic An increase in the SiC etch rate was also obtained by increasing the dc bias voltage, as shown in Fig. 4, which caused increased breakage of SiC bonds at a higher ion bombardment energy, without increasing the F atomic However, this also increased the sputter etch rates of the NiF_x and CuF_x formed on the mask layers. The etch selectivities to Cu and Ni at an etch rate of 1200 nm/min obtained with a dc bias voltage of −600 V, as shown in Fig. 4, are 60 and 40, respectively,

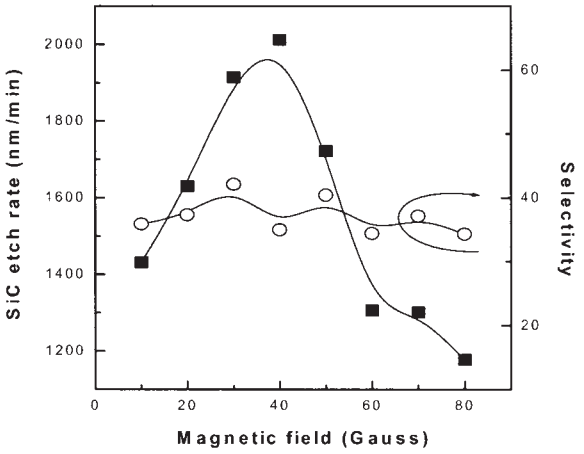

Fig. 6. SiC etch rates and etch selectivities to Ni as a function of the magnetic field at an inductive power of 1400 W, a bias voltage of −600 V, and 10 mTorr of SF_6.

while those to Cu and Ni at 1300 nm/min with a dc bias voltage of −200 V and a magnetic field of 30 G were infinite and 64, respectively. Therefore, for similar SiC etch rates, higher etch selectivities over Cu and Ni can be obtained by the application of a weak magnetic field.

To obtain higher SiC etch rates, the SiC etch rates and their etch selectivities to Ni were measured as a function of the magnetic field from 0 to 80 G for a dc bias voltage of −600 V, and the results are shown in Fig. 6. The applied inductive power and operational pressure were 1400 W and 10 mTorr of SF_6, respectively. As shown in this figure, the change in the SiC etch rate as a function of the magnetic field at a bias voltage of −600 V was similar to that at a bias voltage of −200 V, as shown in Fig. 5(a). However, the maximum SiC etch rate in the presence of an axial magnetic field of 40 G increased to 2020 nm/min. The etch selectivity over Ni at a dc bias voltage of −600 V did not change significantly with the application of a magnetic field and remained near 40. In the case of Cu, at the high SiC etch rate conditions afforded by the application of a magnetic field of nearly 40 G, the Cu mask layer was removed faster than the Ni one. As shown in Figs. 4 and 5(a), through the application of a higher dc bias voltage and magnetic field, the etch rates of the Cu and Ni mask layers become close to each other. When both a high dc bias voltage of −600 V and a magnetic field of 40 G were used, the Cu mask layer appeared to have a mixed surface layer consisting of Cu and CuF_x, as shown in Fig. 3, possibly due to the heavy ion bombardment. Due to the higher Cu sputter etch rate compared to that of Ni, and possibly due to the etching of bare Cu before the formation of a thick copper fluoride layer, caused by the high sputter rates, the Cu mask having a mixed surface layer of Cu and CuF_x appears to have a lower etch selectivity compared to the Ni mask. Therefore, Cu does not appear to be suitable as the etch mask for the high etch rate conditions shown in Fig. 6, even though it appears to be a good etch mask for low etch rate conditions.

4. Conclusion

In this study, using magnetized inductively coupled plasmas, the etch rates of SiC and the etch selectivities to Cu and Ni were studied for the fluorinated gases, CF_4, NF_3, and SF_6, as functions of the inductive power, bias voltage and magnetic field strength. The characteristics of the plasmas were investigated using OES and QMS.

Increasing the inductive power and bias voltage increased the SiC etch rates, due to the resulting increase in the F atomic density in the plasma and ion bombardment energy, respectively. SF_6 showed the highest SiC etch rates and etch selectivities to Cu and Ni among the gases investigated in our study, due to the higher F atomic density obtained in this case and the formation of nonvolatile fluoride on Cu and Ni. Cu generally showed higher etch selectivity than Ni, possibly due to the easier formation of copper fluoride, as compared to the formation of nickel fluoride in the case of Ni. At a fixed inductive power and bias voltage, the application of an axial magnetic field of up to 40 G increased the SiC etch rate approximately two times, and this increase in the etch rate was related to the further increase in the F atomic density and ion densities in the plasma. However, the increase in the SiC etch rate was accompanied by a decrease in the etch selectivity to Cu and Ni. The highest SiC etch rate obtained in our experiment was 2020 nm/min with an inductive power of 1400 W, a bias voltage of −600 V, a pressure of 10 mTorr of SF_6, and a magnetic field of 40 G. Under these conditions, the etch selectivity to Ni was about 40, however, the etch selectivity to Cu was lower, due to the increased sputtering of Cu which occurred before the formation of copper fluoride at a bias voltage of −600 V.

Acknowledgments

This work was supported by the National Research Laboratory Program of the Korea Ministry of Science and Technology.

1) K. Xie, J. H. Zhao, J. R. Flemish, T. Burke, W. R. Buchwald, G. Lorenzo and H. Singh: IEEE Electron Device Lett. **17** (1996) 142.
2) R. J. Trew, J. Yan and P. M. Mock: Proc. IEEE **79** (1991) 598.
3) L. Cao, B. Li and J. H. Zhao: J. Electrochem. Soc. **145** (1998) 3609.
4) P. H. Yih, V. Saxena and A. J. Steckl: Phys. Status Solidi B **202** (1997) 605.
5) J. R. Flemish, K. Xie and G. F. McLane: Mater. Res. Soc. Symp. Proc. **421** (1996) 153.
6) F. A. Khan, L. Zhou, V. Kumar and I. Adesida: J. Electrochem. Soc. **149** (2002) G420.
7) J. R. Flemish and K. Xie: J. Electrochem. Soc. **143** (1996) 2620.
8) P. Chabert, N. Proust, J. Perrin and R. W Boswell: Appl. Phys. Lett. **76** (2000) 2310.
9) S. M. Kong, H. J. Choi, B. T. Lee, S. Y. Han and J. L. Lee: J. Electron Mater. **31** (2002) 209.
10) H. Cho, K. P. Lee, P. Leerungnawarat, S. N. G. Chu, F. Ren, S. J. Pearton and C. M. Zetterling: J. Vac. Sci. & Technol. A **19** (2001) 1878.
11) J. Hong, R. J. Shul, L. Zhang, L. F. Lester, H. Cho, Y. B. Hahn, D. C. Hays, K. B. Jung, S. J. Pearton, C. M. Zetterling and M. Ostling: J. Electrochem. Soc. **28** (1999) 196.
12) J. J. Wang, E. S. Lambers, S. J. Pearton, M. Ostling, J. M. Grow, F. Ren and R. J. Shul: Solid-State Electron. **43** (1998) 2283.
13) F. A. Khan and I. Adesida: Appl. Phys. Lett. **75** (1999) 2268.
14) F. A. Khan, B. Roof, L. Zhou and I. Adesida: J. Electron Mater. **30** (2001) 212.
15) *XPS Handbook* eds. J. F. Moulder, W. F. Stickle, P. E. Sobol and K. D. Bomben (Physical Electronics, Minnesota, 1995).